PHYSICAL REVIEW VOLUME 107, NUMBER 6 SEPTEMBER 15, 1957

Penetration of Electron Beams into Water below the Critical Energy*

I. ADAWI†
Engineering Physics Department, Cornell University, Ithaca, New York

(Received April 23, 1957)

The "moments technique" has been applied to the calculation of the spatial distribution of the energy dissipation in water by electron beams of energies 10–25 Mev. A continuous energy loss is assumed and the energy-range relationships are obtained taking into account the ionization and radiation losses. These relationships are introduced in the proper Boltzmann transport equation to approximate the scattering term by a simple function of residual range. The stopping power is approximated by a sum of powers of residual range. This leads to expressing the spatial moments of the energy dissipation as a combination of triple moments of the electron distribution function. These triple moments are the angular, spatial, and residual range moments, which are connected by a recursion system. The first three moments are calculated together with the boundary condition and the asymptotic trend. With this information, the distribution is constructed by using a simple analytical function. The agreement with experimental results is satisfactory.

I. INTRODUCTION

THIS work concerns the following problem: A planar monodirectional and monoenergetic source of electrons is embedded in water. We wish to determine the energy dissipated by this electron beam at different depths in the medium.

Spencer[1] (hereafter referred to as SP) has recently succeeded in calculating the distribution of energy dissipation with depth in different media for source energies ranging from a fraction of a Mev to a few Mev. The scheme is to calculate a number of the spatial moments of the distribution in question and then construct the distribution by the "function-fitting" technique[2] already developed in x-ray problems. The functions used are selected to have the same asymptotic trend as that of the energy dissipation, which has been analyzed (SP). The knowledge of the asymptotic trend of the distribution makes it unnecessary to calculate the higher moments and hence guarantees the reliability of the method.

The basic assumption made by Spencer[1] and earlier by Lewis[3] is the continuous-energy-loss approximation. This implies that the energy lost by an electron in a collision, on the average, is much smaller than the electron energy before the collision. Such an assumption is valid when hard collisions are infrequent as in ionization losses by electrons of energies, say, above 0.2 Mev in general. In this case there is a fairly definite energy-range relationship which gives the track length of an electron for a given energy. When the distribution of electrons, of a given energy, with track length is narrow, we say that range straggling is small. But when the bremsstrahlung losses are important, straggling becomes the rule. The reason is that photons of energies comparable to that of the radiating electrons are frequently emitted. The energy-range relationship will have no meaning, then, except in an average sense.

Here we assume the continuous-energy-loss approximation to hold and set as our task the "modification" of Spencer's method to cover higher energies. Since the critical energy for water[4] is about 100 Mev, we are limited to considering energies of the order of 25 Mev where the radiation losses are about $\frac{1}{4}$ of the ionization losses.

In the following sections we shall develop this "modified" method and apply it to calculate the energy dissipation by electron beams of 10–25 Mev in water. The results are compared with the measurements of Skaggs[5] and the agreement is satisfactory.

II. SCATTERING

We adopt the notation of SP and start from his Eq. (6):

$$-\partial I_{ln}/\partial t+S_l(t)I_{ln}(t)=n(2l+1)^{-1}[(l+1)I_{l+1,\,n-1}(t)+lI_{l-1,\,n-1}(t)]+\delta_{n0}\delta(t-1). \quad (1)$$

For the scattering cross section we use the McKinley-Feshbach[6] formula:

$$2\pi\sigma(\beta,\theta)=\tfrac{3}{16}\phi_0 Z(Z+1)(1-\beta^2)\beta^{-4}(\sin^2(\tfrac{1}{2}\theta)+\eta^2)^{-2}\times[1+\pi\alpha\beta Z\sin(\tfrac{1}{2}\theta)-(\beta^2+\pi\alpha\beta Z)\sin^2(\tfrac{1}{2}\theta)],$$
$$\alpha=1/137. \quad (2)$$

The scattering potential is assumed to be of the Yukawa form $(Ze^2/r)\exp(-r/a)$, where a is the screening radius for the Coulomb field of the nucleus. This gives rise to the screening angle 2η given by $\bar{\lambda}/a$, where $\lambda(=2\pi\bar{\lambda})$ is the de Broglie wavelength of the scattered electron.

Dalitz[7] has derived Eq. (2) by using the relativistic Born approximation to second order. This approxima-

---

* Based on a Ph.D. thesis presented to the Faculty of the Graduate School of Cornell University, January, 1957.

† Sigma Xi Fellow (1955–1956). Present address: RCA Laboratories, Princeton, New Jersey.

[1] L. V. Spencer, Phys. Rev. **98**, 1597 (1955).

[2] L. V. Spencer, Phys. Rev. **88**, 801 (1952), Appendix B.

[3] H. W. Lewis, Phys. Rev. **78**, 526 (1950).

[4] W. Heitler, *The Quantum Theory of Radiation* (Oxford University Press, New York, 1954), third edition, pp. 367–377.

[5] L. S. Skaggs, Radiology **53**, 868 (1949).

[6] W. A. McKinley, Jr., and H. Feshbach, Phys. Rev. **74**, 1759 (1948).

[7] R. H. Dalitz, Proc. Roy. Soc. (London) **A206**, 509 (1951).

tion is valid[8] for $Ze^2/\hbar v \ll 1$ which is well satisfied here, since Z for water is less than 8 and $e^2/\hbar v \sim \alpha$ for electrons of a few Mev.

The expression for the collision term, S_l, which is derived from (2) for $\eta l \ll 1$, is

$$S_l(T) = \tfrac{3}{4}\phi_0 Z(Z+1) N r_0 (T+1)^2 T^{-2} (T+2)^{-2} \times \left\{ C_l + 2\pi\alpha\beta Z l - (\beta^2 + \pi\alpha\beta Z) \sum_{i=1}^{l} i^{-1} \right\}, \quad (3)$$

$$C_l = l(l+1) \left\{ \ln\eta^{-1} - \tfrac{1}{2} - \sum_{i=2}^{l} i^{-1} \right\}.$$

This form of C_l is due to Goudsmit and Saunderson.[9] A proof, which is essentially a slight improvement on Bethe's[10] proof, is given in Appendix A. Integrals leading to the remaining terms in (3) are discussed by SP.

In (3), η remains to be specified. This depends intimately on the model used for the electronic structure around the nucleus, and the resulting effect on shielding the nucleus in small-angle collisions. The simplest model is to take a, the screening radius, equal to the Thomas-Fermi radius, namely, $0.885 a_0 Z^{-\frac{1}{3}}$ where a_0 is the first Bohr radius in the hydrogen atom. Commonly η is taken from the Molière calculations[10] based on a Thomas-Fermi potential. However, for low-Z media, Molière's results seem to give smaller screening angles than observed.[10] For the hydrogen atom,[11] $a = a_0/2$ while for oxygen a is of the same order of magnitude. For water, therefore, one can take $a = b a_0/2$, where b can be obtained by comparing (6) with experimental data (if available). In our calculations we have set $a = a_0/2$ for both H and O.

To evaluate a function $N_0 f(Z,\eta)$ for a compound (such as S_l for water) we use the rule:

$$N_0 f(Z,\eta) = \textstyle\sum_i N_i f(Z_i,\eta_i), \quad (4)$$

where N_0 is the number of molecules/g of the compound, N_i is the number of atoms of type i per gram of compound, and Z_i and η_i are the values of Z and η for this type of atom.

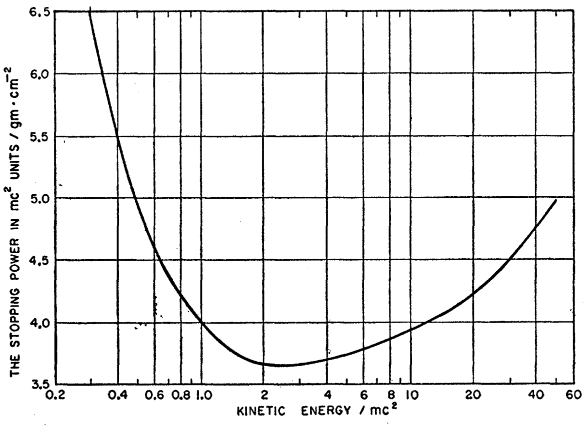

FIG. 1. The stopping power of electrons in water *vs* energy.

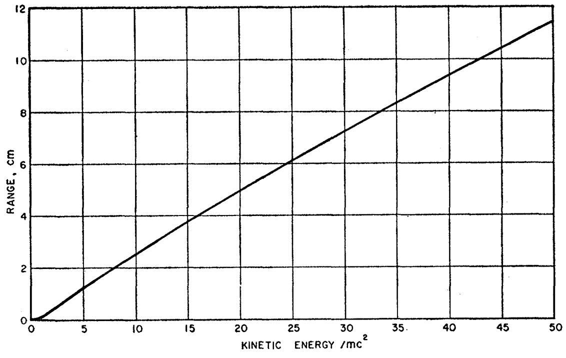

FIG. 2. The range of electrons in water *vs* energy.

III. ENERGY-RANGE RELATIONS

Since the electron energy is dissipated by collision and radiation, we write for the stopping power‡

$$dT/dr = (dT/dr)_{\text{coll}} + (dT/dr)_{\text{rad}}. \quad (5)$$

In calculating the collision loss, we made use of the extensive data given by Sternheimer[12,13] which includes the correction for the "density effect." For water, this effect should be included for electron energies, roughly, above 1 Mev.

The radiation loss is included for electron energies above 5 Mev. The method of calculation is described by Heitler.[4,14]

Once dT/dr is calculated, a simple numerical integral will give the range. The results are presented graphically. Figure 1 shows the stopping power, dT/dr, *versus* kinetic energy T on a semilogarithmic scale. In Fig. 2, the residual range is plotted against T. It is almost a straight line except for small energies where it is nearly parabolic. In Fig. 3, the stopping power is plotted against residual range.

IV. ANALYTIC APPROXIMATIONS

The results of the last section will now be applied to express $S_l(T)$ of Eq. (3) explicitly in terms of residual range, r or t. First we express η in terms of T, and we

---

[8] E. J. Williams, Proc. Roy. Soc. (London) **A169**, 537 (1938–1939).

[9] S. A. Goudsmit and J. L. Saunderson, Phys. Rev. **57**, 24 (1940).

[10] H. A. Bethe, Phys. Rev. **89**, 1256 (1953).

[11] N. F. Mott and H. S. W. Massey, *The Theory of Atomic Collisions* (Clarendon Press, Oxford, 1949), second edition, p. 184.

‡ In this paper, as in SP, T is the kinetic energy in mc^2 units, r the residual range in g/cm², and t is the fraction r/r_0, where r_0 is the initial residual range or simply range. In addition we introduce in Sec. IV $\tau = t + \alpha$, where α is an adjustable parameter, and use it much as SP uses t.

[12] R. M. Sternheimer, Phys. Rev. **88**, 851 (1952).

[13] After the completion of this work, a more recent and slightly modified set of parameters for the density effect has been given by R. M. Sternheimer, Phys. Rev. **103**, 511 (1956).

[14] Reference 4, pp. 252–253.

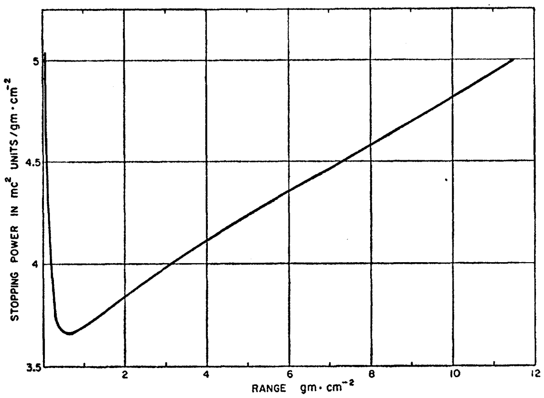

FIG. 3. The stopping power of electrons in water *vs* range.

obtain

$$\eta=\lambda/a_0=\alpha[T(T+2)]^{-\frac{1}{2}}\sim\alpha(T+1)^{-1} \quad \text{for large } T. \tag{6}$$

Using (6) in (3), we observe that the dependence of S_l on T is essentially inverse square multiplied by a slowly varying logarithmic function of T. For low energies, below 1 mc^2, we mentioned that r is parabolic in T, while for high energies it is linear in T. This simple argument suggests that S_l might reduce to d_l/t for low energies and to $d_l/(t^2+ft+g)$ for high energies (where f and g are constants independent of l while d_l depends on l). Indeed, SP finds that for energies up to a few Mev

$$S_l(t)\approx\alpha d_l/[t(t+\alpha)], \tag{7}$$

and that for low energies α is so large that

$$S_l(t)\approx d_l/t. \tag{8}$$

Spencer's calculations are based on these two approximations. The second approximation leads to a simple theory and allows the calculation of a large number of spatial moments of the energy dissipation, while the first leads to a rather complex theory and limits the calculations to a few moments. In fact, for energies above a few Mev, α is so small that the theory does not work at all in practice. The situation is still worse for energies of the order of 20 Mev such as we are considering. This points to a need for a third approximation valid and useful for our range of energies.

Upon tabulating S_1, S_2/S_1, and S_3/S_1 for $1<T<50$, we have found that S_2 and S_3 bear a constant ratio to S_1 to an accuracy of one percent. It was possible to represent S_1 as $d_l/(t+\alpha)^2$ to an accuracy of a few percent. We conclude that

$$S_l\approx d_l/(t+\alpha)^2, \tag{9}$$

which forms the basis of our calculations. In Table I, we give the first three parameters, d_l, together with α for three different energies. In this table $d_2=2.8789d_1$ and $d_3=5.5368d_1$ while α happens to be $0.27/r_0$.

We substitute (9) in (1), then multiply by τ^{p+1} where $\tau=t+\alpha$, and integrate over τ to obtain

$$\begin{aligned}(p+1)I_{ln}{}^{p}+d_lI_{ln}{}^{p-1}=\delta_{n0}(1+\alpha)^{p+1}\\ +n(2l+1)^{-1}\{(l+1)I_{l+1,\,n-1}{}^{p+1}+lI_{l-1,\,n-1}{}^{p+1}\},\end{aligned} \tag{10}$$

where

$$\int_{\alpha}^{1+\alpha}I_{ln}(\tau)\tau^{p}d\tau=I_{ln}{}^{p}.$$

The system (10) is the fundamental recursion system which we shall often use. It can be looked upon as a partial difference equation of the first order in n and second order in l and p. This is in contrast to systems (19) and (25) of SP which are of first order in p.

The energy dissipation distribution, $J(x)$, is given by

$$J(x)=\int_{\alpha}^{1+\alpha}I_0(\tau,x)(dT/d\tau)d\tau, \tag{11}$$

where $dT/d\tau$ can be approximated by

$$dT/d\tau=A_0\tau^{\frac{1}{2}}+A_1+A_2\tau^{-\frac{1}{2}}, \tag{12}$$
$$(A_0=0.72r_0^{\frac{3}{2}},\quad A_1=2.34r_0,\quad A_2=0.626r_0^{\frac{1}{2}})$$

to an accuracy of a few percent for ranges greater than $\frac{1}{4}$ cm. For ranges below 1 millimeter the approximation is not good because $\tau\rightarrow\alpha$ as $t\rightarrow0$ and a finite value for $dT/d\tau$ results when it should, in fact, become infinite. This difficulty could be avoided by adding a delta function to the right-hand side of (12) of proper strength and located, say, at $t=0.1/r_0$. However, we shall see later that this is unnecessary and the difficulty is removed in a natural way without altering the form of Eq. (12).

Using (12) in (11) and taking the nth spatial moment of $J(x)$, we obtain

$$J_n=A_0I_{0n}{}^{\frac{1}{2}}+A_1I_{0n}{}^{0}+A_2I_{0n}{}^{-\frac{1}{2}}. \tag{13}$$

V. CALCULATION OF THE MOMENTS

The moments of interest are to be evaluated in increasing order of n as suggested by (10). Having evaluated the right-hand side of the system (10), we still have to determine one $I_{ln}{}^{P}$ in order to know $I_{ln}{}^{p+k}$ where k is an integer. This is achieved only by quadratures. From Eq. (18) of SP and our approximation (9), we obtain

$$I_{ln}(\tau)=\int_{\tau}^{1+\alpha}d\tau'F_{ln}(\tau')\exp\{d_l(1/\tau'-1/\tau)\}, \tag{14}$$

TABLE I. Scattering parameters.

T	α	d_1	d_2	d_3
23.88	0.04615	0.1847	0.5319	1.02289
32.1	0.03506	0.1404	0.4041	0.7771
40	0.02869	0.1149	0.3306	0.6359

where

$$F_{ln}(\tau)=n(2l+1)^{-1}\{(l+1)I_{l+1,\,n-1}(\tau)+lI_{l-1,\,n-1}(\tau)\}+\delta_{n0}\delta(\tau-1-\alpha).$$

Multiply (14) by τ^p and integrate over τ, then invert the order of integration to obtain the equation,

$$I_{ln}{}^{p}=\int_{\alpha}^{1+\alpha}d\tau' F_{ln}(\tau')\exp(d_l/\tau')\times\int_{\alpha}^{\tau'}d\tau\tau^{p}\exp(-d_l/\tau). \quad (15)$$

Integrate the inner integral in (15) once by parts. A recursion system results which is identical to (10) if the lower limit is stretched to zero, i.e.,

$$I_{ln}{}^{p}=\int_{\alpha}^{1+\alpha}d\tau'\cdots\int_{0}^{\tau'}\cdots d\tau. \quad (16)$$

This explains why we do not have to modify (12).

First Moment

The zeroth moment is simply the total energy loss T. To evaluate J_1, we need to know $I_{01}{}^{p}$ for $p=0$, $\pm\frac{1}{2}$. From (10) and (16) we have:

$$(p+1)I_{01}{}^{p}=I_{10}{}^{p+1}, \quad (17)$$

$$I_{10}{}^{p+1}=\exp\{d_1(1+\alpha)^{-1}\}\int_{0}^{1+\alpha}d\tau\tau^{p+1}\exp(-d_1/\tau). \quad (18)$$

The integral (18) is elementary. It reduces to the error function for half-integral values of p and to the exponential integral for integral values of p. The result of these calculations is:

$$I_{01}{}^{-\frac{1}{2}}=\tfrac{4}{3}\{(1+\alpha)^{\frac{3}{2}}-2d_1(1+\alpha)^{\frac{1}{2}}+2\pi^{\frac{1}{2}}d_1{}^{\frac{3}{2}}\exp[d_1(1+\alpha)^{-1}]\,\mathrm{erfc}[d_1/(1+\alpha)]^{\frac{1}{2}}\}, \quad (19)$$

$$I_{01}{}^{\frac{1}{2}}=\frac{2}{15}\{2(1+\alpha)^{\frac{5}{2}}-d_1I_{01}{}^{-\frac{1}{2}}\}, \quad (20)$$

$$I_{01}{}^{0}=\tfrac{1}{2}\{(1+\alpha)^2-d_1(1+\alpha)+d_1{}^2\exp[d_1/(1+\alpha)]E[d_1(1+\alpha)^{-1}]\}, \quad (21)$$

where

$$\mathrm{erfc}x\equiv1-\mathrm{erf}x\equiv2\pi^{-\frac{1}{2}}\int_{x}^{\infty}\exp(-x^2)dx,$$

$$E(x)\equiv-\mathrm{Ei}(-x)\equiv\int_{x}^{\infty}(dx/x)\exp(-x).$$

The moments given by (19)–(21) are combined according to (13) and J_1 is thus obtained.

Second Moment

To calculate J_2 we have to know $I_{02}{}^{p}$ for $p=0$, $\pm\frac{1}{2}$. From (10), it follows that

$$(p+1)I_{02}{}^{p}=2I_{11}{}^{p+1}, \quad (22)$$

and the problem reduces to calculating $I_{11}{}^{p}$ for integral and half-integral value of p. For convenience we select $p=-1$ and $-\frac{3}{2}$. Using (16), we derive:

$$I_{11}{}^{-1}=\int_{\alpha}^{1+\alpha}d\tau F_{11}(\tau)\exp(d_1/\tau)E(d_1/\tau), \quad (23)$$

$$I_{11}{}^{-\frac{3}{2}}=\pi^{\frac{1}{2}}d_1{}^{-\frac{1}{2}}\int_{\alpha}^{1+\alpha}d\tau F_{11}(\tau)\exp(d_1/\tau)\,\mathrm{erfc}(d_1/\tau)^{\frac{1}{2}}, \quad (24)$$

where

$$F_{11}(\tau)=\tfrac{1}{3}\{2\exp[d_2\{(1+\alpha)^{-1}-1/\tau\}]+1\}.$$

These integrals are evaluated as discussed in Appendix B. The system (10) is then used to give $I_{02}{}^{0}$ and $I_{02}{}^{\pm\frac{1}{2}}$ from which J_2 is obtained.

All the calculations were carried out on a desk calculator. No moments higher than the second have been attempted because of their increasing complexity.

VI. DISTRIBUTION

In constructing the distribution $J(x)$, we include the boundary condition and the asymptotic trend, in addition to the first three moments we have just calculated.

According to SP, the asymptotic trend is given by

$$J(x)\sim(1-x)^{-\frac{3}{2}}\exp\{-A/(1-x)\}. \quad (25)$$

However, we shall here assume this trend to have the conjectured empirical form,

$$J(x)\sim(1-x)^{\gamma}\exp\{-A/(1-x)\}, \quad (26)$$

of which (25) is a special case.

We shall assume $J(x)=0$ for $x<0$ since the scattering is highly in the forward direction for these energies. The boundary condition is

$$J(0)=dT/dt,\quad t=1. \quad (27)$$

The distribution is constructed by using the simple function, $g(x)$, given by

$$g(x)=J(0)(1-x)^{\gamma}\exp\{a^2[1-(1-x)^{-1}]\}. \quad (28)$$

The function $g(x)$ satisfies the boundary condition (27) and behaves asymptotically as $J(x)$ in (26). The parameters γ and a^2 are varied so that the first two moments of $g(x)$, namely, g_0 and g_1, agree with J_0 and J_1, respectively. The second moment J_2 is compared with g_2 to check on the accuracy of this particular form of representation. It was found that γ is close to $-\frac{1}{2}$. On taking $J(0)$ to be unity, we obtain

$$J(x)\approx g(x)=(1-x)^{-\frac{1}{2}}\exp\{a^2[1-(1-x)^{-1}]\}. \quad (29)$$

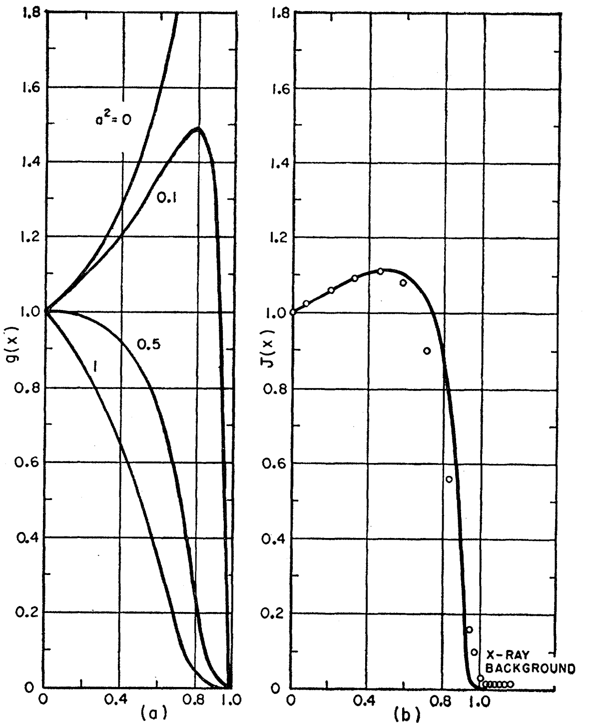

FIG. 4. (a) The function $g(x)$ for different values of a^2. (b) The function $J(x)$ for 16.4 Mev. The measurements of Skaggs are shown in circles.

The moments of $g(x)$ are elementary. The first three are

$$\begin{aligned} g_0&=2\{1-a\pi^{\frac{1}{2}}\exp(a^2)\operatorname{erfc}a\},\\ g_1&=g_0(1+\tfrac{2}{3}a^2)-\tfrac{2}{3}, \\ g_2&=g_0[1+\tfrac{4}{3}a^2+(4/15)a^4]-(14/15)-(4/15)a^2. \end{aligned} \tag{30}$$

The moments g_n satisfy the recursion system,

$$0=ng_{n-1}-(2n+\tfrac{3}{2}+a^2)g_n+(n+\tfrac{3}{2})g_{n+1}. \tag{31}$$

For large n,

$$g_n\sim(\pi/n)^{\frac{1}{2}}\exp(a^2-2an^{\frac{1}{2}}). \tag{32}$$

Now we discuss the behavior of $g(x)$ in the interval, $0\leqslant x\leqslant 1$. In Fig. 4(a), $g(x)$ is plotted for $a^2=0, \frac{1}{10}, \frac{1}{2}$, and 1 to illustrate all the possible shapes which $g(x)$ can assume within the range of interest; $g(x)$ assumes a peak at $x=1-2a^2$. For small a, the peak is sharp and lies close to $x=1$. As a increases, the peak broadens, decreases in height, and moves to the left. For $a^2>\frac{1}{2}$ the peak does not appear in the range of interest and $g(x)$ decreases monotonically as illustrated by the curve $a^2=1$.

From this discussion, it is evident that by selecting the form (28) as a possible representation of $J(x)$, we have not made any restrictions on the shape of the approximating function. We have not demanded from $g(x)$ to be always of a transition character (unimodal), i.e., rising to a peak and then dropping off. It is a which determines the shape of the curve; that can only be determined by fitting moments.

VII. RESULTS

Our calculations gave $a^2=0.22$, 0.24, and 0.26 for the energies 12.2, 16.4, and 20.4 Mev, respectively. The energy-dissipation curves for all these energies are unimodal with a broad peak. Figure 4(b) shows $g(x)$ for 16.4 Mev as calculated from this theory. The measurements of Skaggs[5] are shown in circles for comparison. The agreement is satisfactory when we consider the semiempirical nature of these calculations and the experimental difficulties encountered in the measurements. In Skaggs' arrangement, the beam is only uniform to within 10% and travels a distance equivalent to about 0.6 cm of water before it enters the water phantom. We have corrected for this fact by extrapolating Skaggs' curve to the left by 0.6 cm.

It is of interest to know the depth at which the maximum energy dissipation occurs and also the ratio of this maximum to the initial value, $J(0)$. In Fig. 5 we present the available data on the position of this peak and its ratio to $J(0)$. The points shown fall in three categories: (a) the results of this theory for 12.2, 16.4, and 20.4 Mev, (b) the dose-depth measurements of Skaggs for 12.2, 14.3, and 16.4 Mev, (c) the measurements of Trump[15] and his colleagues for low energies up to 1.5 Mev (can be calculated as in SP).

In concluding, we point out that this theory can be applied for electron energies of the order of $\frac{1}{10}$ to $\frac{1}{4}$ of the critical energy for the medium considered. Water has been selected for illustration.

The limitations of this theory are similar to that of SP for "intermediate energies" [based on approximation (7)], in that one can calculate in practice only a few moments of the distribution.

ACKNOWLEDGMENTS

It is a pleasure to thank Professor P. Morrison for suggesting the problem to me and for many valuable

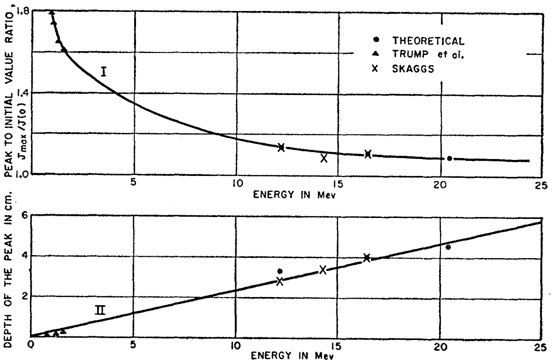

FIG. 5. Curve I gives the ratio $J_{\max}$ to $J(0)$. Curve II shows the depth at which $J(x)$ is maximum.

---

[15] Trump, Van de Graaf, and Cloud, Am. J. Roentgenol. Radium Therapy 43, 728 (1940).

discussions and much advice. Dr. L. V. Spencer and Mrs. Nelms of the National Bureau of Standards have supplied us with a useful table on stopping power and residual range for which we wish to thank them. The author is grateful to Cornell University for the fellowships he was awarded.

APPENDIX A. THE GOUDSMIT-SAUNDERSON (GS) FORMULA

From the definition given by GS[9] and Bethe's[10] scheme (Eq. 81), C_l is given by

$$C_l=\int_{-1}^{1-\epsilon} dx(1-x)^{-2}[1-p_l(x)]. \tag{A.1}$$

Bethe performs a partial integration to obtain

$$C_l=\tfrac{1}{2}\{l(l+1)-1-P_l(-1)\}+\int_{-1}^{1-\epsilon} dx(1-x)^{-1}P_l'(x). \tag{A.2}$$

It follows from (A.2) that

$$C_l+C_{l-1}=l^2-1+\int_{-1}^{1-\epsilon} dx\{p_l'(x)+p_{l-1}'(x)\}(1-x)^{-1}. \tag{A.3}$$

Inserting in (A.3) the recursion formula,

$$p_l'(x)+p_{l-1}'(x)=l(1-x)^{-1}\{p_{l-1}(x)-p_l(x)\},$$

and using (A.1), we obtain the recursion system,

$$F_l-F_{l-1}=-1/l, \quad l>1$$

where

$$F_l=C_l/\{l(l+1)\}. \tag{A.4}$$

This immediately yields the GS formula,

$$C_l=l(l+1)\left\{\tfrac{1}{2}C_1-\sum_{i=2}^{l} i^{-1}\right\}. \tag{A.5}$$

By a simple integration, $C_1\approx 2\ln\eta^{-1}-1$ for the Yukawa potential.

APPENDIX B. INTEGRALS OF THE SECOND MOMENT

I_{11}^{-1}

In (23) let

$$d_1/\tau=y;\quad d_1/\alpha=y_2,\quad d_1(1+\alpha)^{-1}=y_1,$$

$$d_2-d_1=cd_1 \quad (c=1.8789 \text{ Table I, Sec. IV}),$$

and it follows that

$$I_{11}^{-1}=\tfrac{1}{3}d_1\{2A\exp[d_2(1+\alpha)^{-1}]+B\}, \tag{B.1}$$

where

$$A=\int_{y_1}^{y_2} dyy^{-2}E(y)\exp(-cy), \tag{B.2}$$

$$B=\int_{y_1}^{y_2} dyy^{-2}E(y)\exp y. \tag{B.3}$$

Integrate (B.2) by parts twice to obtain

$$A=\Big\{-y^{-1}E(y)\exp(-cy)+y^{-1}\exp[-(c+1)y]-(c+1)E[(c+1)y]\Big\}_{y_1}^{y_2}-c\int_{y_1}^{y_2} dyy^{-1}E(y)\exp(-cy). \tag{B.4}$$

B can be reduced similarly, but it is better to set $c=-1$ in (B.4) to obtain B, since B is equal to A for $c=-1$. Thus,

$$B=\Big\{-y^{-1}E(y)\exp y+y^{-1}\Big\}_{y_1}^{y_2}+\int_{y_1}^{y_2} dyy^{-1}E(y)\exp y. \tag{B.5}$$

From Table I of Sec. IV, we see that y_1 is of the order of $\frac{1}{10}$ and y_2 is about 4. The integrands in (B.4) and (B.5) vary rapidly near the lower limit and are unsuitable, in this form, for numerical quadrature. We split the range of integration into two parts at $y=1$. Calling the integrals in (B.4) and (B.5) A' and B', we have

$$A'=\left\{\int_{y_1}^{1}+\int_{1}^{y_2}\right\}dyy^{-1}E(y)\exp(-cy), \tag{B.6}$$

$$B'=\left\{\int_{y_1}^{1}+\int_{1}^{y_2}\right\}dyy^{-1}E(y)\exp y. \tag{B.7}$$

The last integrals on the right of (B.6) and (B.7) are simple to handle numerically. As for the first integrals, the rapid variation near the lower limit is removed by the artifice of adding and subtracting the leading terms in the expansions of the exponential and the exponential integral functions. The added terms are integrated terms and the subtracted terms are retained under the integral sign to smooth the integrand. Thus

$$\int_{y_1}^{1} dyy^{-1}E(y)\exp(-cy)$$

$$=\int_{y_1}^{1} dyy^{-1}\{E(y)\exp(-cy)-(-\gamma-\ln y)(1-cy+\tfrac{1}{2}c^2y^2)\}+\Big\{-\gamma\ln y+c\gamma y-\tfrac{1}{4}\gamma c^2y^2-\tfrac{1}{2}(\ln y)^2+cy(\ln y-1)-\tfrac{1}{4}c^2y^2(\ln y-\tfrac{1}{2})\Big\}_{y_1}^{1}, \tag{B.8}$$

where $\gamma=$ Euler constant $=0.577216\cdots$, and $-\gamma-\ln y$ are the leading terms in the expansion of $E(y)$. The integral in (B.8) is now simple to evaluate numerically to four figures by Simpson's or Weddle's rule using intervals of width 0.1 for example.

Setting $c=-1$ in (B.8), we reduce the first integral in B' to a suitable form. Once A' and B' are evaluated, it is an easy matter to collect terms and compute A and B from which $I_{11}{}^{-1}$ follows.

$I_{11}{}^{-\frac{3}{2}}$

In (24), let

$$d_1/\tau=x^2,\quad (d_1/\alpha)^{\frac{1}{2}}=x_2,\quad d_1^{\frac{1}{2}}(1+\alpha)^{-\frac{1}{2}}=x_1;$$
$$d_2-d_1=cd_1,$$

and we obtain

$$I_{11}{}^{-\frac{3}{2}}=\tfrac{4}{3}(\pi d_1)^{\frac{1}{2}}\exp[d_2(1+\alpha)^{-1}]C+\tfrac{2}{3}(\pi d_1)^{\frac{1}{2}}D,\qquad\text{(B.9)}$$

where

$$C=\int_{x_1}^{x_2}dx x^{-3}\operatorname{erfc}x\exp(-cx^2),\qquad\text{(B.10)}$$

$$D=\int_{x_1}^{x_2}dx x^{-3}\operatorname{erfc}x\exp x^2.\qquad\text{(B.11)}$$

C and D are now reduced by applying two partial integrations. The result is:

$$C=\Big\{-\tfrac{1}{2}x^{-2}\exp(-cx^2)\operatorname{erfc}x+x^{-1}\pi^{-\frac{1}{2}}\exp[-(c+1)x^2]$$
$$+(c+1)^{\frac{1}{2}}\operatorname{erf}[(c+1)^{\frac{1}{2}}x]+\tfrac{1}{2}cE(cx^2)\Big\}_{x_1}^{x_2}$$
$$+\int_{x_1}^{x_2}dx x^{-1}\exp(-cx^2)\operatorname{erf}x,\qquad\text{(B.12)}$$

$$D=\Big\{-\tfrac{1}{2}x^{-2}\exp(x^2)\operatorname{erfc}(x)+x^{-1}\pi^{-\frac{1}{2}}+\tfrac{1}{2}\operatorname{Ei}(x^2)\Big\}_{x_1}^{x_2}$$
$$-\int_{x_1}^{x_2}dx x^{-1}\exp x^2\operatorname{erf}x,\qquad\text{(B.13)}$$

where

$$\operatorname{Ei}(x)=\int_{-\infty}^{x}dx x^{-1}\exp x.$$

The integral of (B.12) is now simple to evaluate numerically; that of (B.13) will be expressed as a power series.

By definition,

$$\operatorname{erf}x=2\pi^{-\frac{1}{2}}\int_0^x dx\exp(-x^2).\qquad\text{(B.14)}$$

Integrate (B.14) once by parts to obtain

$$\operatorname{erf}x=2\pi^{-\frac{1}{2}}\left(x\exp(-x^2)+\int_0^x 2dx x^2\exp(-x^2)\right).$$

Repeating this process of partial integrations, we derive the formula

$$\operatorname{erf}x=2\pi^{-\frac{1}{2}}\exp(-x^2)x\sum_{n=0}^{\infty}\frac{(2x^2)^n}{3\cdot5\cdot7\cdots(2n+1)}.\qquad\text{(B.15)}$$

Substituting (B.15) in (B.13) and integrating term by term, we obtain

$$\int_{x_1}^{x_2}dx x^{-1}\operatorname{erf}x\exp(x^2)$$
$$=2\pi^{-\frac{1}{2}}\sum_{n=0}^{\infty}\frac{(2x^2)^n}{3\cdot5\cdot7\cdots(2n+1)(2n+1)}\Bigg]_{x_1}^{x_2}.\qquad\text{(B.16)}$$

This series is convergent for all finite values of x. The error committed by summing a reasonable finite number of terms is of the order of the first term neglected (as can be seen by ratio tests for example). For $x=0.6$ the sum of five terms differs from that of the series by about 10^{-10}. For $x=2$, the sum of about twenty terms is needed to give the same accuracy.

Once C and D are evaluated, as sketched above, they are combined according to (B.9) to give $I_{11}{}^{-\frac{3}{2}}$.